COMPARISON OF HYBRID-POL DESCRIPTORS FROM MULTI-SENSOR POLARIMETRIC SAR DATA

Vineet Kumar, Dipankar Mandal, Y. S. Rao
Centre of Studies in Resources Engineering,
Indian Institute of Technology Bombay, India 400076

ABSTRACT

Proposed work aims to compare the effect of different frequencies and incident angles on hybrid polarimetric descriptors. The test site selected for this study is San Francisco area. L-band (AIRSAR and ALOS-2/PALSAR-2) and C-band (RADARSAT-2 and RISAT-1) data are collected for this study. The hybrid-pol descriptors such as the degree of polarization (*DoP*), Relative phase (*Delta*) and ellipticity angle (*Chi*) have been extracted for comparision.

The analysis has been performed by taking around 10,000 pixels (100 x100 window) of urban and sea areas. These two classes are selected as their scattering response is closer to the dihedral and trihedral targets respectively. For AIRSAR L-band data, the distribution peak of *DoP*, *Delta* and *Chi* are around 0.98, $+90^0$ and $+40^0$ for sea area pixels. However, in urban areas, the distribution peak is around 0.80, -75^0 and -21^0. In the ideal case, the values for a dihedral point target (dihedral CR) is 1.0, -90^o, -45^0. The reason for the difference is due inhomogeneity in the urban areas. Similar values are obtained with ALOS-2 data.. However, the peaks of the histogram deviate from AIRSAR results. With C-band RADARSAT-2 simulated hybrid-pol data, no clear peak is observed for *Delta* in urban areas. The delta values of large pixels are found in the range of -90^0 to -85^0. The real hybrid-pol data from RISAT-1 satellite shows peak histogram for *DoP*, *Delta* and *Chi* around 0.65, -60^0, -5^0 in Urban areas. The results indicate that hybrid-pol descriptors are sensitive to the change in frequency and incidence angle of the transmitted wave.

KEYWORDS*:* *Hybrid polarimetry, RISAT-1, Stokes Vector*

1. INTRODUCTION

In compact polarimetry, only one polarization is transmitted and two orthogonal polarizations are received. Compact polarimetry SAR systems retain the relative phase between two received waves. The term compact polarimetry alternatively used for the transmission of three different kinds of polarizations; these are the $\pi/4$ mode, dual circular pol (DCP) and hybrid-pol mode (Souyris et al., 2005). The hybrid mode of compact polarimetry refers to transmission of any circularly (left or right) polarized wave and reception of two orthogonal linearly (H&V) polarized signal. Sometime this mode is also known as circular transmit and linear receive (CTLR) mode. The hybrid polarimetry mode provides a trade of between transmitted power and swath of the data (Raney 2007). Existing quad pol data obtained from full pol airborne and satellite platforms can also be simulated to any dual circular or hybrid pol mode. Hybrid/compact polarimetry offers several advantages over full polarimetry in terms of lower data rate, wider swath, less PRF, low power consumption and simpler antenna configuration (Charbonneau et al., 2010). The importance of hybrid-pol parameters obtained from Stokes vector is shown for various application such as oil spill (Haiyan li et al., 2015) and ship detection (Shirvany et al., 2012), sea-ice detection (Daboor et al., 2014, Singha et al, 2017), agriculture (Ballester-Berman & Lopez-Sanchez, 2012) and soil moisture applications (Ponnurangam et al., 2016). The utility of relative phase (*delta*) from Stokes vector is shown for compact-pol phase calibration, feature detection (Raney 2007) and wind turbines identification in the ocean (Haiyan li et al., 2013). Haiyan et al., also show that the *delta* is not affected by the wind speed and incidence angle changes. However, when the transmitted wave is not perfectly circular, ellipticity angle (*chi*) is considered as a robust parameter to use (Raney et al., 2012). The estimation of the degree of polarization (*DoP*) and its application for feature identification is given in Shirvany et al., 2013. Similar to quad-pol decomposition, in hybrid polarimetry, model based decomposition has been proposed to understand the scattering from targets. The basic component of hybrid-pol decomposition is also double-bounce, surface and random scattering. In this study, a comparative assessment has been made to see the effect of frequency and incidence angle on hybrid-pol parameters obtained from different SAR sensors. As the SAR data is collected on different dates, the comparison of the results may not be ideal.

2. STUDY AREA AND DATASET

The SAR datasets are collected from airborne and space borne platforms over the San Francisco Bay area, USA. The detailed characteristics of SAR data used in this study are given in Table 1. AIRSAR and RADARSAT-2 images used in this study are freely available to download in quad-pol mode. L-band AIRSAR image is in STK-MLC format with image size of 900 x 1024 rows and columns. RISAT-1 is the first SAR satellite operating in hybrid-pol mode for earth observation applications. The fine resolution stripmap-1 (FRS-1) SLC image of RISAT-1 is acquired for this study in hybrid-pol. The right circular transmission and linear H & V-pol reception facility are available in RISAT-1 hybrid-pol data. ALOS-2/PALSAR-2 and RADARSAT-2 SLC images are collected in quad-pol mode. The simulation of hybrid-pol data is possible through existing quad-pol data. Details of the hybrid-pol simulation from full-pol are given in the following section. ALOS-2/PALSAR-2 and RISAT-1 images are acquired on the same date, i.e. August 09, 2016 over the San Francisco Bay area. Urban areas, water body and vegetation, are the major land use land cover (LULC) in the area.

Table 1: Satellite data acquisition date and parameters

Date DD/MM/YY	Satellite	Incidence angle	Pass Type/Look
09/08/2016	ALOS-2	30.40^0	Ascending/Right
09/08/2016	RISAT-1	38.19^0	Ascending/Left
09/04/2008	RADARSAT-2	28.50^0	Ascending/Right

3. METHODOLOGY

By considering a coherent dual-polarized right circularly transmitted SAR, the four Stokes parameters in linear received polarization basis can be defined in eq. 1-4 (Raney et al., 2012). Where $\langle ... \rangle$ represents the ensemble average, * is a complex conjugate product, and RH/RV are right circular transmit and linear H & V received.

$$S_1 = \langle |E_{RH}|^2 + |E_{RV}|^2 \rangle \quad (1)$$

$$S_2 = \langle |E_{RH}|^2 - |E_{RV}|^2 \rangle \quad (2)$$

$$S_3 = 2Re\langle E_{RH} E_{RV}^* \rangle \quad (3)$$

$$S_4 - 2Im\langle E_{RH} E_{RV}^* \rangle \quad (4)$$

The first Stokes parameter (S_1) is proportional to the total power of received wave. Stokes second parameter (S_2) gives information about the polarization, whether it is more vertical or horizontal. The third (S_3) and fourth (S_4) terms represents the phase difference between the received polarizations. Left or right-handedness of circular can also be determined by fourth Stokes parameter.

As already mentioned that it is possible to simulate hybrid-pol data from existing quad-pol. The four Stokes parameters can be derived from 3x3 covariance [C3] (Raney 2007) or coherency matrix [T3] (Cloude et al., 2012). The formulation of [S_1, S_2, S_3 and S_4] from [T3] matrix is given in eq. 5. The upper (+) and lower (-) indicates left hand and right-hand circular polarization respectively.

$$\begin{bmatrix} S_1 \\ S_2 \\ S_3 \\ S_4 \end{bmatrix} = \begin{bmatrix} \frac{1}{2}(t_{11} + t_{22} + t_{33}) \pm Im(t_{23}) \\ Re(t_{12}) \pm Im(t_{13}) \\ Re(t_{13}) \mp Im(t_{12}) \\ Im(t_{23}) \pm \frac{1}{2}(t_{22} + t_{33} - t_{11}) \end{bmatrix} \quad (5)$$

From these four stokes parameters; it is possible to derive the secondary hybrid-pol parameters such degree of polarization (*DoP*), relative phase (*delta*) and ellipticity angle (*chi*).

Degree of polarization (*DoP*) = $m = \frac{\sqrt{S_2^2 + S_3^2 + S_4^2}}{S_1}$ $\quad 0 \leq m \leq 1$ (6)

Ellipticity (*chi*) = $\chi = \frac{1}{2}\sin^{-1}(-S_4/mS_1)$ $\quad -45^0\ \chi \leq +45^0$ (7)

Relative phases = $\delta = \text{atan}(\frac{S_4}{S_3})$ $-180^0\ \delta \leq 180^0$ (8)

Except for RISAT-1 satellite data, which is already acquired in hybrid-pol, for all other sensors Stokes parameters are simulated from quad-pol data. The preprocessing steps for quad-pol data involve multi-looking and coherency matrix [T3] generation followed by speckle removal (Refined LEE filter, window: 5x5). Stokes vector is generated from the [T3] matrix as given in eq. 5. RISAT-1 data is multilooked at the time of 2x2 covariance [C2] matrix generation. Inherent speckle noise of RISAT-1 data is suppressed by applying Refined LEE filter of window 5x5. Stokes vector has been generated from [C2] matrix followed by hybrid-pol parameter extraction from RISAT-1 data.

4. RESULTS AND DISCUSSION

The *DoP*, *delta* and *chi* parameters are extracted from different SAR datasets. For this, an approximately common region of interest (ROI) is drawn over water body (sea) and built up areas (mainly building and roads) in the study area. The analysis has been performed by taking around 10,000 pixels (100 x100 window) of urban and sea areas. These two classes are selected as their scattering response is closer to the dihedral and trihedral targets. Figure 1 shows the RGB colour composite image over the study area. Built up areas, ocean surface and vegetation features can be seen clearly.

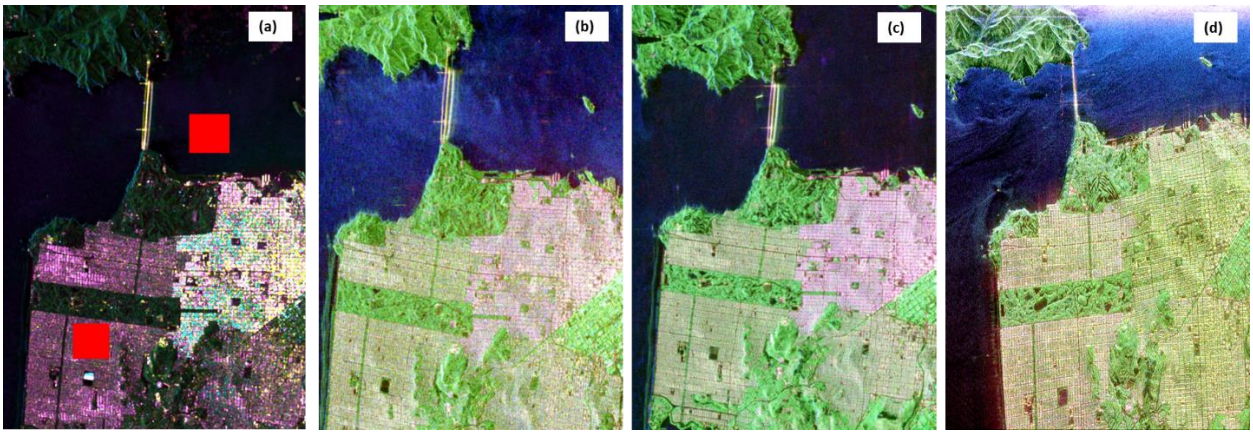

Figure 1. Pauli RGB colour composite image over the San Francisco Bay area for four different sensors (a) RISAT-1 Raney RGB (b) RADARSAT-2 (c) ALOS-2/PALSAR-2 (d) AIRSAR. Red Boxes indicates the region of interest taken for analysis.

4.1 Hybrid-pol Parameters for Ocean Surface

Figure 2 shows *DoP*, *delta* and *chi* parameters extracted from the sea surface in row 1, 2 and 3 respectively. *DoP* is very important parameter to characterize partially polarized wave. For RISAT-1, the peak of *DoP* histogram can be observed near to 0.6, whereas for RADARSAT-2 its closer to 0.9. The peak of *DoP* histogram for L-band ALOS-2 and AIRSAR is around 0.7 and 0.98 respectively. It has been observed as that the *DoP* values are confined to the very narrow range of values and variance is very low. The relative phase (*delta*) for the trihedral or odd bounce type of target should be closer to $+90^0$. The peak of histograms for different SAR systems in Figure. 2 shows that *delta* peaks are 90^0 in AIRSAR, ALOS-2 and RADARSAT-2 data. However, for RISAT-1 it is around 106^0. The number of pixels from ocean surface are also concentrated in a narrow range for AIRSAR and RADARSAT-2, whereas for RISAT-1 and ALOS-2 the pixels are distributed over a wider range. The received ellipticity angle histogram shows that peak is near to 40^0 for AIRSAR data, 32^0 for ALOS-2 data, 37^0 for RADARSAT-2 and 28^0 for RISAT-1 data. The variance in the distribution of ellipticity angle is also observed higher in RISAT-1 and ALOS-2 compared to the AIRSAR and RADARSAT-2 data. The major reason for the difference among SAR sensors and deviation from ideal value is the distributed nature of targets and sensor look direction and incidence angle. The ideal values mentioned are for point targets. However, backscattering from ocean surface and urban areas is the combination of scattering from multiple targets within pixel. Another probable cause of deviation in RISAT-1 data is the non-circularity of the transmitted signal. The comparison of RISAT-1 and ALOS-2 histograms for all the hybrid parameters in Figure 2 shows that effect of frequency as well as incident angle on these descriptors as both the images are acquired on the same date.

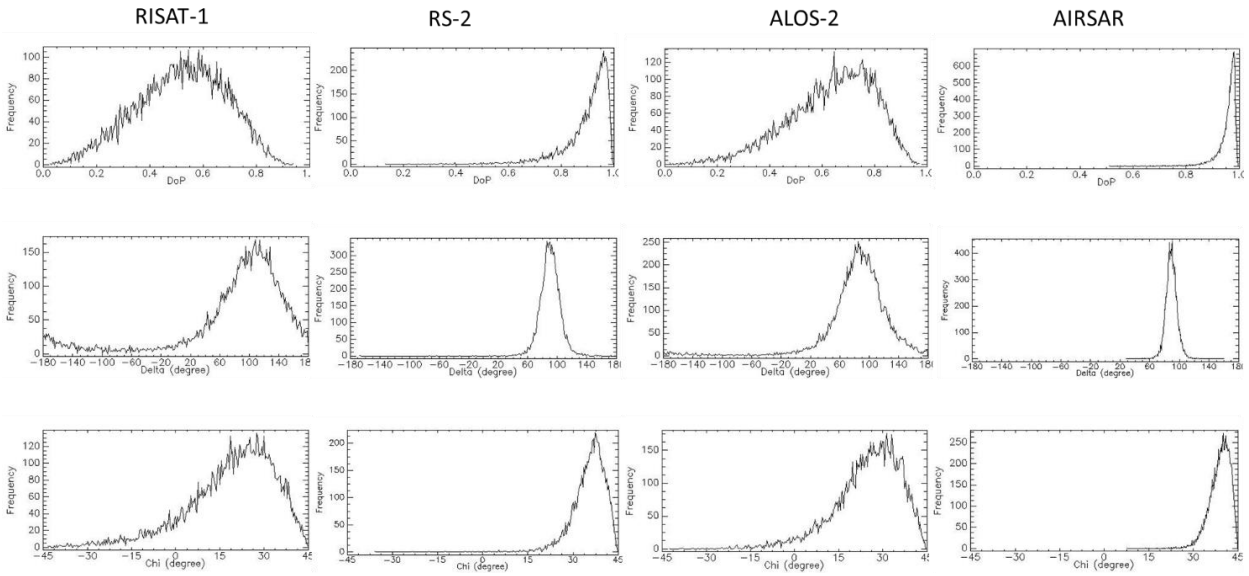

Figure 2. Histograms of DoP (first row), Delta (second row) and Chi (third row) over water area (sea surface) of San Francisco area for different SAR data sets.

4.2 Hybrid-pol Parameter for Urban areas

The response of hybrid parameters over urban area is shown in Figure 3. The Urban ROIs mainly consist of built-up area and roads. The *DoP*, *Delta* and *Chi* plots are not smooth for urban areas as compared to ocean observations. This is mainly due to the homogeneity of the ocean surface in comparison to urban features. This can be observed in the plots of *DoP* values, where histogram peak can be seen at around 0.6 for RISAT-1 and ALOS-2. The histogram peak for RADARSAT-2 and AIRSAR is near to 0.8. The relative phase (*delta*) peaks come in negative value range which is an indicator of double bounce scattering from Urban targets. Effect of radar signal frequency can be seen on the histogram of the *delta*. A clear peak is observed in the histogram of L-band ALOS-2 and AIRSAR data near -45^0 and -80^0, whereas in C-band RISAT-1 and RADARSAT-2 a clear peak of the *delta* is not visible. However, the maximum value of *delta* is occurred at -48^0 for RISAT-1 and at -88^0 for RADARSAT-2 data.

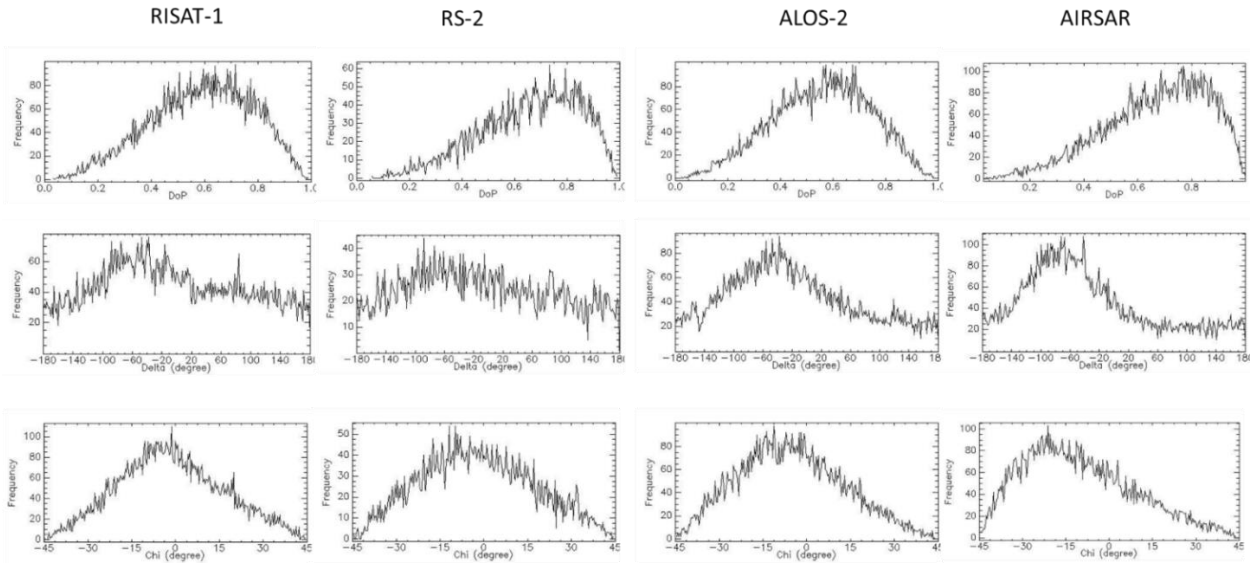

Figure 3. Histograms of DoP (first row), Delta (second row) and Chi (third row) over Urban areas of San Francisco area for different SAR data sets.

The one probable causes of similarity between RISAT-1 and ALOS-2 derived hybrid-pol parameters almost same of time of data acquisition. Hence, Urban features are almost in the same state on these acquisition dates. However, there may be few chances of different wind conditions over the ocean surface.

5. CONCLUSION

The result obtained from this study indicates that hybrid-pol parameters such as *DoP*, *delta* and *chi* can distinguish the ocean surface with urban areas. The distributed nature of targets and non-circularity of the transmitted wave may be the reason for the shift in the histogram peaks from ideal values. The results indicate that hybrid-pol descriptors are sensitive to the change in frequency and incidence angle of the transmitted wave. The best way one can compare different SAR systems using using dihedral and dihedral corner reflectors response.

6. ACKNOWLEDGEMENT

The authors acknowledge the JPL-NASA, USA and MDA for freely providing AIRSAR and RADARSAT-2 data respectively. ALOS-2 PALSAR-2 data is provided by JAXA through RS-6. RISAT-1 is acquired through ISRO-IITB sponsored project.

REFERENCES

Ballester-Berman, J. D., & Lopez-Sanchez, J. M. (2012). Time series of hybrid-polarity parameters over agricultural crops. IEEE Geoscience and Remote Sensing Letters, 9(1), 139-143.

Charbonneau, F.J., Brisco, B., Raney, R.K., McNairn, H., Liu, C., Vachon, P.W., Shang, J., DeAbreu, R., Champagne, C., Merzouki, A. and Geldsetzer, T., 2010. Compact polarimetry overview and applications assessment. *Canadian Journal of Remote Sensing*, *36*(S2), pp.S298-S315.

Cloude, S.R., Goodenough, D.G. and Chen, H., 2012. Compact decomposition theory. *IEEE Geoscience and Remote Sensing Letters*, *9*(1), pp.28-32.

Dabboor, M. and Geldsetzer, T., 2014. Towards sea ice classification using simulated RADARSAT Constellation Mission compact polarimetric SAR imagery. Remote sensing of environment, 140, pp.189-195.

Li, H., Perrie, W., He, Y., Lehner, S. and Brusch, S., 2013. Target detection on the ocean with the relative phase of compact polarimetry SAR. *IEEE Transactions on Geoscience and Remote Sensing*, *51*(6), pp.3299-3305.

Li, H., Perrie, W., He, Y., Wu, J. and Luo, X., 2015. Analysis of the polarimetric SAR scattering properties of oil-covered waters. *IEEE Journal of Selected Topics in Applied Earth Observations and Remote Sensing*, *8*(8), pp.3751-3759.

Ponnurangam, G.G., Jagdhuber, T., Hajnsek, I. and Rao, Y.S., 2016. Soil moisture estimation using hybrid polarimetric SAR data of RISAT-1. *IEEE Transactions on Geoscience and Remote Sensing*, *54*(4), pp.2033-2049.

Raney, R.K., 2007. Hybrid-polarity SAR ar*chi*tecture. *IEEE Transactions on Geoscience and Remote Sensing*, *45*(11), pp.3397-3404.

Raney, R.K., Cahill, J.T., Patterson, G. and Bussey, D.B.J., 2012. The m-*chi* decomposition of hybrid dual-polarimetric radar data with application to lunar craters. *Journal of Geophysical Research: Planets*, *117*(E12).

Shirvany, R., Chabert, M. and Tourneret, J.Y., 2012. Ship and oil-spill detection using the degree of polarization in linear and hybrid/compact dual-pol SAR. IEEE Journal of Selected Topics in Applied Earth Observations and Remote Sensing, 5(3), pp.885-892.

Shirvany, R., Chabert, M. and Tourneret, J.Y., 2013. Estimation of the degree of polarization for hybrid/compact and linear dual-pol SAR intensity images: Principles and applications. *IEEE Transactions on Geoscience and Remote Sensing*, *51*(1), pp.539-551.

Singha, S. and Ressel, R., 2017. Arctic Sea Ice Characterization Using RISAT-1 Compact-Pol SAR Imagery and Feature Evaluation: A Case Study Over Northeast Greenland. *IEEE Journal of Selected Topics in Applied Earth Observations and Remote Sensing (under pagination)*.

Souyris, J.C., Imbo, P., Fjortoft, R., Mingot, S. and Lee, J.S., 2005. Compact polarimetry based on symmetry properties of geophysical media: The/spl pi//4 mode. IEEE Transactions on Geoscience and Remote Sensing, 43(3), pp.634-646.